International Journal of Numerical Methods for Heat & Fluid Flow

Emerald Article: Solution of a low Prandtl number natural convection benchmark by a local meshless method

þÿ G r e g o r K o s e c , B o ~ i d a r ` a r l e r

The current issue and full text archive of this journal is available at
www.emeraldinsight.com/0961-5539.htm

Solution of a low Prandtl number natural convection benchmark by a local meshless method

Gregor Kosec
Laboratory for Parallel and Distributed Computing, Jožef Stefan Institute, Ljubljana, Slovenia and
Laboratory for Multiphase Processes, University of Nova Gorica, Nova Gorica, Slovenia, and
Božidar Šarler
Laboratory for Multiphase Processes, University of Nova Gorica, Nova Gorica, Slovenia and
Laboratory for Advanced Materials Systems, Centre of Excellence for Biosensorics, Automation and Process Control, Solkan, Slovenia

Received 29 February 2012
Revised 18 September 2012
Accepted 25 September 2012

Abstract

Purpose – The purpose of this paper is to present the solution of a highly nonlinear fluid dynamics in a low Prandtl number regime, typical for metal-like materials, as defined in the call for contributions to a numerical benchmark problem for 2D columnar solidification of binary alloys. The solution of such a numerical situation represents the first step towards understanding the instabilities in a more complex case of macrosegregation.

Design/methodology/approach – The involved temperature, velocity and pressure fields are represented through the local approximation functions which are used to evaluate the partial differential operators. The temporal discretization is performed through explicit time stepping.

Findings – The performance of the method is assessed on the natural convection in a closed rectangular cavity filled with a low Prandtl fluid. Two cases are considered, one with steady state and another with oscillatory solution. It is shown that the proposed solution procedure, despite its simplicity, provides stable and convergent results with excellent computational performance. The results show good agreement with the results of the classical finite volume method and spectral finite element method.

Originality/value – The solution procedure is formulated completely through local computational operations. Besides local numerical method, the pressure velocity is performed locally also, retaining the correct temporal transient.

Keywords Numerical methods, Fluids, Convection, Newtonian incompressible fluid, Low Prandtl number, Natural convection, Rectangular cavity, Primitive variables, Meshless methods, Local radial basis function collocation method, Multiquadrics, Local pressure-correction

Paper type Research paper

The research was funded through Slovenian state research projects J2-4120, P2-0379 and P2-0095. The Centre of Excellence for Biosensors, Instrumentation and Process Control is an operation financed by the European Union, European Regional Development Fund and Republic of Slovenia, Ministry of Higher Education, Science and Technology. The financial support is kindly acknowledged.

International Journal of Numerical Methods for Heat & Fluid Flow
Vol. 23 No. 1, 2013
pp. 189-204

0961-5539
DOI 10.1108/09615531311289187

1. Introduction

The computational modelling of solidification has become an important research subject due to its pronounced influence in better understanding of nature as well as in the development of the advanced technologies. The main computational difficulties in tackling solidification systems stem from the moving interface between the solid and the liquid phase, respective jump of the physical properties (density, viscosity, etc.) across the interface as well as possible jumps in heat flux, species flux and concentration at the interface. The jumps are accompanied by the fast thermal diffusion compared to the species diffusion, and involved convection phenomena. The convection phenomena arise due to the thermal and solutal gradients in the melt as well as convection, triggered through the movement of the interface between the solid and the liquid phase with different densities. The situation could be additionally complicated by the surface tension governed (Marangoni) convection, and movement of the dispersed solid phase, that might be present in the melt. The respective flow patterns can be laminar, periodic or turbulent. The computational treatment of solidification phenomena can be conducted on different scales that might range from the dendritic growth on the micron scale (Lorbiecka and Šarler, 2010), grain growth on the millimeter scale, and system level on the meter scale (Vertnik *et al.*, 2011). It is a long term vision to be able to solve the grain size and distribution of the solidified system, microsegregation (chemical inhomogeneities) on the scale of the solidified grain, and macrosegregation (chemical inhomogeneities) on the system level, together with a range of segregations on the length scales between micro and macro.

There have been many computational studies performed up to now to simulate the macrosegregation. However, a precise answer on how accurate the results are (verification of macrosegregation modelling) is quite a novel issue, proposed in a recent benchmark test by Bellet *et al.* (2009). This benchmark test, that logically follows the melting exercise, proposed by Gobin and Le Quéré (2000) consists of two parts. I. A separate preliminary single phase exercise: concerned with the convective problem in the absence of solidification and in conditions close to those met in solidification processes. Two problems are considered for the case of laminar natural convection: I. a transient thermal convection for a pure liquid metal with a Prandtl number of the order of 10^{-2}, and I. b double-diffusive convection in an enclosure for a binary liquid metallic mixture with a Prandtl number on the order of 10^{-2} and a Lewis number on the order of 10^{-4}. II. The simulation of the full solidification process: first a specified "minimal" solidification model is proposed with II. a Pb-18%Sn and II. b Sn-10%Pb alloys. The objective is to compare the numerical solutions obtained by different contributors (verification). Then different physical solidification models may be compared to check the features that allow for the best possible prediction of the physical phenomena (validation). It is essential for proper simulation of macrosegregation to be able to simulate the transient natural convection and the double-diffusive flow structure. The part I.a of the proposed benchmark is tackled in the present work, which by the best of knowledge of the present authors represents the first results achieved on this benchmark.

Natural convection heat transfer problems are fully determined through Rayleigh and Prandtl dimensionless numbers. Rayleigh number stands for the ratio between the buoyant to the viscous effects, and depends also on the geometry and boundary conditions. The Prandtl number, defined as the ratio of the momentum diffusivity to the thermal diffusivity, is an intrinsic thermophysical property of a fluid, which is not

directly dependent on the problem configuration. The Prandtl number varies over several orders of magnitude from 10^{-3} (liquid metals) to 10^{5} (functional oils) in common fluids. Ratio between Prandtl and Rayleigh numbers is also known as Grashof number, which characterises the flow regime. There are three important values of the Grashof number which demarcate different flow bifurcations in a specific natural convection arrangement. The first critical value denotes the onset of steady convection from the conduction regime, the second one the onset of the periodic convection from the steady convection, and the third one the onset of the turbulent convection from the periodic convection. Subsequently, the effects of geometry, boundary conditions and fluid properties continue to attract the computational fluid dynamics community in search for more and more accurate as well as diverse simulations of natural convection (Amimul, 2011).

Before tackling the macrosegregation as a consequence of the solidification of binary substance, a proper solution of natural convection, double-diffusive convection and freezing, is needed. Detailed analyses and accurate solutions of different stages of solidification will maximize the possibilities to identify the differences between different numerical solutions at the point when they might originate. A comparison study of solution of macrosegregation, computed with the finite volume method and the finite element method (with quite different qualitative and quantitative response of different numerical method simulations) already exists, however there was until now no effort given to reasonably systematic identification of the origin of the differences in both solutions (Ahmad *et al.*, 1998).

The defined (Bellet *et al.*, 2009) macrosegregation cases with Pb-18%Sn and Sn-10%Pb give as a consequence results with mesosegragates which seem, at the moment, difficult to calculate in a discretisation and numerical method independent way. We have recently defined a related macrosegregation case, free of mesosegregates, and most probably for the first time demonstrated mesh independent and numerical method independent results (Kosec *et al.*, 2011). The numerical methods used were the finite volume method and the local radial basis function collocation method (LRBFCM) (Kosec and Šarler, 2008).

The transient natural convection of the low Prandtl number fluids in 2D was probably for the first time studied in archival literature by Mohamad and Viskanta (Mohamad and Viskanta, 1991). Their work follows a number of technical reports, cited in their paper. They numerically caught periodic oscillations at the critical Grashof numbers. Prior to the oscillatory flow, the steady state solutions with an oscillatory transient period were numerically predicted. The effect of boundary conditions and time marching schemes on the Mohamad and Viskanta reference solutions has been further studied by (Cless and Prescott, 1996a, b). A 3D study of Rayleigh-Benard convection of a low-Prandt-Number fluid in shallow 3D cavity heated from below was studied in Nakano *et al.* (1998). All mentioned studies used the finite difference method solution procedure. The work of Mohamad and Viskanta was recalculated by the finite element method in 1999 (Sammouda *et al.*, 1999). A problem of a low Prandtl number natural convection in volumetrically heated rectangular enclosures was studied for different situations by Arcidiacono and Ciofalo (2001), Arcidiacono *et al.* (2001) and Di Piazza and Ciofalo (2001). A comparison between the finite volume method and the spectral Chebyshev method (Xin and Le Quere, 2002), for low Prandtl number natural convection in a shallow cavity was given by Založnik *et al.* (2005). The transition from steady to

oscillatory flow for a very low Prandtl number fluid (Pr = 0.008) was studied for rectangular enclosures with aspect ratios (length/height) of 0.25, 0.4, 1.0 and 2.0 by Crunkleton *et al.* (2006) with the finite volume method and SIMPLE pressure correction algorithm. A graph of Rayleigh number of first bifurcation of natural convection was recently given for a range of Prandtl numbers from 0.1 to 1.0 in Xiaohua *et al.* (2009). Tesso and Piva (Pesso and Piva, 2009) recently calculated the low Prandtl natural convection in a square cavity, caused by large differences in the working fluid, characterised by the Gay-Lussac number (Ga) in addition to the Ra and Pr. They used a finite volume based commercial software for obtaining the steady state results for a range of Pr from 0.0071 to 0.71, Ra from 10 to 10^8 and Ga from 0 to 2. Finally the authors propose a heat transfer correlation for the tackled range of situations.

The meshless or sometimes also named meshfree or mesh reduction methods represent a class of numerical methods where an arbitrarily distributed set of nodes, without any additional topological relations between them, is used. Such meshless methods represent a promising technique to avoid problems with polygonisation. There exist several meshless methods such as element free Galerkin method, the Meshless Petrov-Galerkin method, the point interpolation method, the point assembly method, the finite point method, smoothed particle hydrodynamics method, reproducing kernel particle method, Kansa method (Monaghan, 1988; Kansa, 1990a, b; Atluri and Shen, 2002a, b; Chen, 2002; Liu, 2003; Gu and Liu, 2005; Fasshauer, 2006; Šterk and Trobec, 2008; Trobec *et al.*, 2009). However, this work is focused on one of the simplest classes of meshless methods in development today, the local point interpolation (Wang and Liu, 2002) radial basis function (Buhmann, 2000) collocation method (RBFCM) (Šarler, 2007). Undoubtedly, these methods can be of great advantage in solving solidification processing problems. In the present paper we use a local variant of RBFCM (Šarler, 2007), the LRBFCM. The main advantage of the local approach is that the spatial disretization problem is simplified to solving small systems instead of large global systems, which might become unstable for increasing number of computational nodes. The LRBFCM approach was already successfully applied to several thermo-fluid situations, ranging from the laminar to turbulent situations (Šarler and Vertnik, 2006; Vertnik and Šarler, 2006; Divo and Kassab, 2007; Kosec and Šarler, 2008).

2. Governing equations

The considered problem domain is a closed air-filled square-shaped cavity with differentially heated vertical walls with temperature difference ΔT and insulated horizontal walls. The non-permeable and no-slip velocity boundaries are assumed. The problem is described by three coupled PDE equations: mass (equation (1)), momentum (equation (2)) and energy conservation (equation (3)) equations, where all material properties are considered to be constant. The Boussinesq approximation (equation (4)) is used for the treatment of body force in the momentum equation. The natural convection is thus described by the following system of equations:

$$\nabla \cdot \mathbf{v} = 0, \tag{1}$$

$$\rho \frac{\partial \mathbf{v}}{\partial t} + \rho \nabla \cdot (\mathbf{v}\mathbf{v}) = -\nabla P + \nabla \cdot (\mu \nabla \mathbf{v}) + \mathbf{b}, \tag{2}$$

$$\rho \frac{\partial (c_p T)}{\partial t} + \rho \nabla \cdot (c_p T \mathbf{v}) = \nabla \cdot (\lambda \nabla T), \tag{3}$$

$$\mathbf{b} = \rho[1 - \beta_T(T - T_{\text{ref}})]\mathbf{g}. \tag{4}$$

with $\mathbf{v}$, P, T, λ, c_p, $\mathbf{g}$, ρ, β_T, T_{ref}, μ and $\mathbf{b}$ standing for velocity, pressure, temperature, thermal conductivity, specific heat, gravitational acceleration, density, coefficient of thermal expansion, reference temperature for Boussinesq approximation, viscosity and body force, respectively. The case is characterised by three dimensionless numbers:

$$\text{Ra}_T = \frac{|\mathbf{g}|\beta_T \Delta T \Omega_H^3 \rho^2 c_p}{\lambda \mu} \tag{5}$$

$$\text{Pr} = \frac{\mu c_p}{\lambda}, \tag{6}$$

$$\text{A} = \frac{\Omega_H}{\Omega_W}, \tag{7}$$

standing for Rayleigh number, Prandtl number and domain aspect ratio. The ratio between Rayleigh and Prandtl is often referred as Grashof number, defined as:

$$\text{Gr} = \frac{\text{Ra}_T}{\text{Pr}}. \tag{8}$$

Ω_H stands for domain height and Ω_W for domain width (Figure 1).

The introduced physical model does not have a closed form solution and in order to solve it a numerical approach has to be employed. A reference eponymous work in this field is that by de Vahl Davis (1983).

3. Solution procedure

In this paper we use a novel local meshless numerical method with local pressure-velocity coupling. A general idea behind the local meshless methods is the use of local

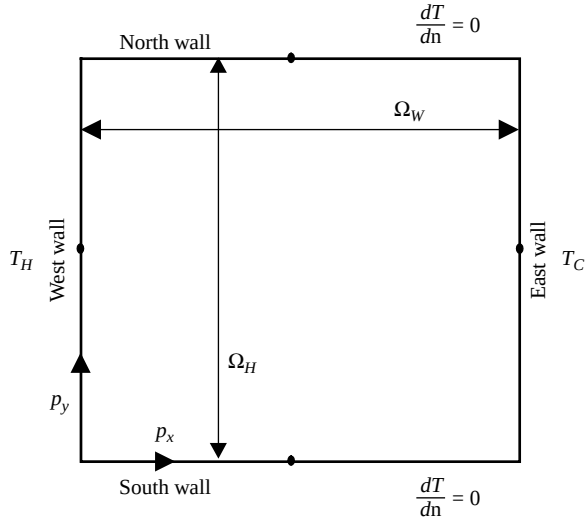

Figure 1.
The natural convection benchmark test schematics

sub clusters of domain nodes (Figure 2), named local support domains, with local basis functions for the approximation of fields. With the selected support domain, an approximation function is introduced as a sum of weighted basis functions:

$$\theta(\mathbf{p}) = \sum_{n=1}^{N_{Basis}} \alpha_n \Psi_n(\mathbf{p}), \tag{9}$$

where θ, N_{Basis}, α_n and Ψ_n stand for the approximation function, the number of basis functions, the approximation coefficients and the basis functions, respectively. The basis could be selected arbitrarily (e.g. monomials, radial basis function, etc.), however in this paper Hardy's multiquadrics (MQs):

$$\Psi_n(\mathbf{p}) = \sqrt{(\mathbf{p} - \mathbf{p}^n) \cdot (\mathbf{p} - \mathbf{p}^n)/\sigma_C^2 + 1}, \tag{10}$$

with σ_C standing for the free shape parameter of the basis function, are used, based on the results of the study by Franke (1982). By taking into account all support domain nodes and equation (9) the approximation system is obtained. In this paper we use collocation (the number of support nodes is the same as the number of the basis functions). An arbitrary spatial differential operation (L) can be applied on the approximation function in the following way:

$$L\theta(\mathbf{p}) = \sum_{n=1}^{N_{Basis}} \alpha_n L\Psi_n(\mathbf{p}). \tag{11}$$

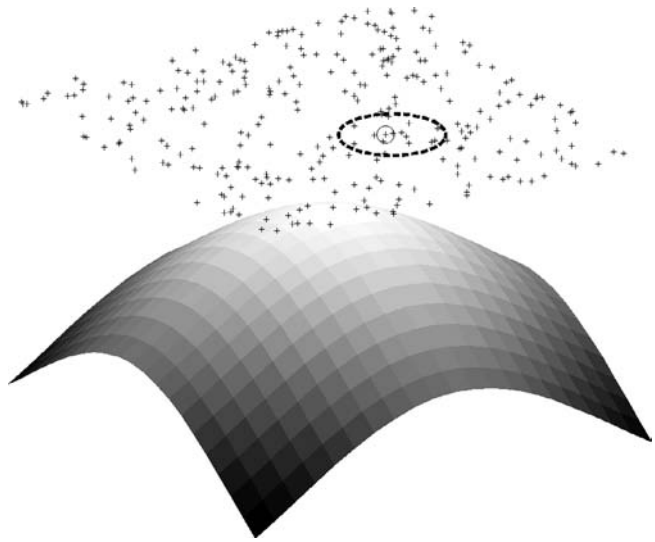

Note: The differential operations in a circled node are performed only through the consideration of a local influence domain

Figure 2.
Schematic representation of meshless numerical principle

In general, the system (9) has to be solved only when the influence domain topology changes and therefore the computation can be optimized by computing $\boldsymbol{\Psi}^{-1}$ in a pre-process. Furthermore, the computation of the coefficients and the evaluation of differential operators can be combined. All information about the numerical approach and the local nodal topology can be stored in a predefined vector, which has to be re-evaluated only when the topology of the nodes changes. The differential operator vector $\left(\chi_m^L\right)$ is introduced as:

$$\chi_m^L(\mathbf{p}) = \sum_{n=1}^{N} \Psi_{nm}^{-1} L(\Psi_n(\mathbf{p})) \tag{12}$$

The introduced formalism holds in general and therefore the general notation for partial differential operator (L) is used. However, in the present work, only operators $\partial/\partial p_\varepsilon$ and ∇^2 are employed:

$$\chi_m^{\nabla^2}(\mathbf{p}) = \sum_{n=1}^{N} \Psi_{nm}^{-1} \sum_{\varepsilon} \frac{\partial^2}{\partial p_\varepsilon^2} \Psi_n(\mathbf{p}), \tag{13}$$

$$\chi_m^{\partial/\partial p_\varepsilon}(\mathbf{p}) = \sum_{n=1}^{N} \Psi_{nm}^{-1} \frac{\partial}{\partial p_\varepsilon} \Psi_n(\mathbf{p}), \tag{14}$$

The structured formulation is convenient since most of the complex and CPU demanding operations are performed in the pre-process phase. For all inner temporal loop operations only N floating point operations (FLOPS) are need for evaluation of an arbitrary partial differential operator. The implementation of the Dirichlet boundary condition is straightforward. In order to implement Neumann and Robin boundary conditions a special case of interpolation is needed. In these boundary nodes the function directional derivative instead of the function value is known and therefore the equation in the interpolation system changes to:

$$\theta_{BC} = \sum_{n=1}^{N_{Basis}} \alpha_n \left(a \frac{\partial}{\partial \mathbf{n}} \Psi_n(\mathbf{p}) + b \Psi_n(\mathbf{p}) \right). \tag{15}$$

In the presented numerical framework the computation of Neumann and Robin boundary conditions can be simplified through the usage of the differential operator vector. Consider the Neumann boundary condition:

$$a \frac{\partial \theta}{\partial \mathbf{n}} + b\theta = \theta_{BC}, \tag{16}$$

$$\theta_0 = \frac{\theta_{BC} - a \sum_{m=2}^{N_{Sub}} \chi_m^{\partial/\partial \mathbf{n}} \theta_m}{a \chi_0^{\partial/\partial \mathbf{n}} + b}, \tag{17}$$

where θ_0 stands for boundary node. Equation (17) simplifies to Neumann boundary condition computation if b is set to zero. Such approach makes the Neumann and the Robin boundary condition computation straightforward and CPU effective, again only N flops are needed to evaluate it, without any kind of special computational treatment on or near boundaries.

For the temporal discretization we use a two-level explicit time stepping:

$$\rho_0 \frac{\theta - \theta_0}{\Delta t} = \nabla \cdot (D_0 \nabla \theta_0) - \nabla \cdot (\rho_0 \mathbf{v}_0 \theta_0) + S_0, \tag{18}$$

where zero-indexed quantities stand for the values at the initial time, and D, S for general diffusion coefficient, and source term, respectively. The time step is denoted with Δt. The pressure-velocity coupling is performed through the correction of the intermediate velocity ($\hat{\mathbf{v}}$):

$$\hat{\mathbf{v}} = \mathbf{v}_0 + \frac{\Delta t}{\rho}(-\nabla P_0 + \nabla \cdot (\mu \nabla \mathbf{v}_0) + \mathbf{b}_0 - \nabla \cdot (\rho \mathbf{v}_0 \mathbf{v}_0)) \tag{19}$$

Equation (19) did not take into account the mass continuity and respective corrections need to be applied:

$$\hat{\mathbf{v}}^{m+1} = \hat{\mathbf{v}}^m + \widehat{\mathbf{v}}, \tag{20}$$

$$\hat{P}^{m+1} = \hat{P}^m + \widehat{P}, \tag{21}$$

where m, $\widehat{v}$ and $\widehat{P}$ stand for iteration index, velocity correction and pressure correction, respectively. By combining the momentum and the mass continuity equations, the pressure correction Poisson equation emerges:

$$\nabla \hat{\mathbf{v}}^m = \frac{\Delta t}{\rho} \nabla^2 \widehat{P}. \tag{22}$$

Instead of solving the global Poisson equation exactly, the pressure correction is guessed from the divergence of the intermediate velocity:

$$\widehat{P} = \ell^2 \frac{\rho}{\Delta t} \nabla \cdot \hat{\mathbf{v}}^m. \tag{23}$$

The proposed assumption makes solving of the pressure-velocity coupling iteration local. Such an approach is very CPU efficient, as it needs only one computation for each pressure correction. With the computed pressure correction the pressure and the velocity can be corrected as:

$$\hat{P}^{m+1} = \hat{P}^m + \zeta \widehat{P}, \tag{24}$$

where ζ stands for the relaxation parameter. The iteration is performed until the criterion $\nabla \cdot \hat{\mathbf{v}} < \varepsilon_V$ is met in all computational nodes. The approach is similar to the artificial compressibility method (ACM) (Massarotti *et al.*, 1998; Rahman and Siikonen, 2008) and in the framework of the finite difference method to the SOLA approach (Hong, 2004). However, the proposed approach retains the correct time transient which is not the case in SOLA and ACM approaches. The free fluid flow situations have been tackled by ACM in Traivivatana *et al.* (2007) and the flow in porous media in Malan and Lewis (2011). In the present paper we are particularly interested in proper transient response of the computations. The proposed solution procedure is effective from computational point of view as all numerical operations are completely local. Despite several degrees of freedom over the spatial discretization, its complexity remains comparable to finite difference method or finite volume method.

4. Numerical results

The results of the benchmark tests are assessed in terms of streamfunction and cavity Nusselt number, with dimensionless variables, defined as:

$$\tilde{p}_x = \frac{p_x}{\Omega_W} \quad \tilde{p}_y = \frac{p_y}{\Omega_H}, \tag{25}$$

$$\tilde{v}_x = \frac{v_x \Omega_W \rho c_p}{\lambda} \quad \tilde{v}_y = \frac{v_y \Omega_H \rho c_p}{\lambda}, \tag{26}$$

$$\tilde{T} = \frac{T - T_C}{T_H - T_C}, \tag{27}$$

$$\tilde{t} = \frac{\lambda}{\rho c_p \Omega_H^2}\, t. \tag{28}$$

$$\tilde{\psi}(\tilde{\mathbf{p}}) = \int_0^1 \tilde{v}_x(\tilde{\mathbf{p}}) d\tilde{p}_y, \tag{29}$$

$$\mathrm{Nu}(\tilde{\mathbf{p}}) = -\frac{\partial \tilde{T}(\tilde{\mathbf{p}})}{\partial \tilde{p}_x} + \tilde{v}_x(\tilde{\mathbf{p}})\tilde{T}(\tilde{\mathbf{p}}). \tag{30}$$

The Nusselt number is computed locally on five nodded influence domains, while the streamfunction is computed on the 1D influence domains representing each row, where all nodes in the row are used as an influence domain. The streamfunction is set to zero in south west corner of the domain $\tilde{\psi}(0, 0) = 0$. The presented solution procedure is first verified through the comparison of results against previously published data. The similar oscillatory low Prandtl number flow is considered, where a tall cavity with height/width aspect ratio $A = 4$ is filled with $Pr = 0.0137$ (Al4.5%Cu alloy) fluid and simulated at $Ra = 2.81 \cdot 10^5$. Current numerical approach is compared against finite volume method and Chebishev spectral method (Založnik *et al.*, 2005). In present paper the results are presented in terms of hot side mean Nusselt number and its transformation into frequency domain (Figure 4). From Figure 4 it can be seen that our present numerical approach shows good agreement with more standard numerical solutions. In the present work computation is performed on 40,497 uniformly distributed nodes. This case has already been solved in Divo and Kassab (2007) and Kosec and Šarler (2009). We additionally present the frequency analysis of the case in the present paper. In Figure 3 the streamlines and the temperature contour plots for tall cavity test at different times are presented.

The numerical setup of present cases is presented in Table I together with some characteristic results of numerical solution. Dimensionless pressure-velocity coupling relaxation parameter is set to the same numeric value as a dimensionless time step in all computations. The dimensionless pressure-velocity coupling criterion $\tilde{\varepsilon}_V$ is set to 0.5 for all computations. Free RBF shape parameter σ_C is set to 90 in all computations. In our computations case 1 results in steady state while case 2 produces oscillatory solution. In Table I the maximum streamfunction and hot side mean Nusselt numbers in steady state are presented for case 1. For case 2 the values averaged over $\tilde{t} \in [5, 7]$ are stated. Figure 4 shows excellent agreement of the present method with the FEM and spectral method. Solution of case 1 is shown in Figure 5, where the streamlines and the temperature contour

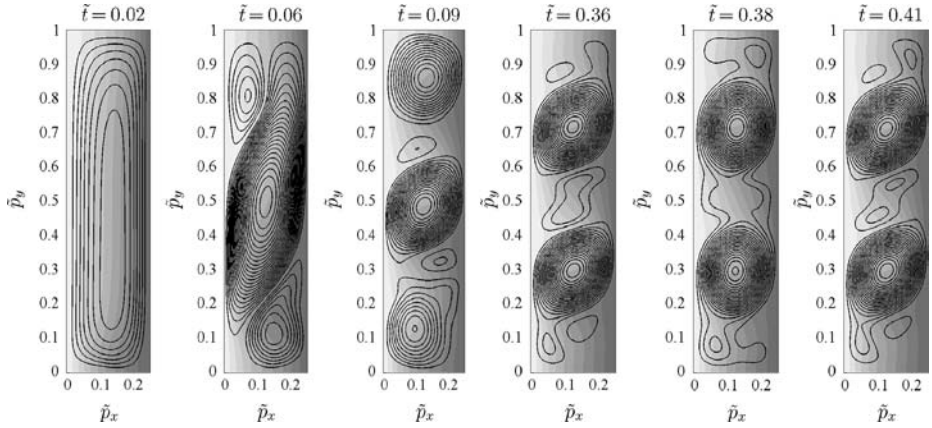

Figure 3.
Streamlines (stream step 0.2) and temperature contours (contour step 0.1) for tall cavity test

	Ra	Pr	A	N_D	$d\tilde{t}, \zeta$	$\tilde{\psi}_{max}$	$Nu_{mean}^{hot\ side}$	
Case 1	10^4	0.01	1	437	10^{-4}	4.3358	2.0615	Steady state values
				2,597	$5 \cdot 10^{-5}$	4.4735	1.9496	
				10,197	10^{-5}	4.5896	1.9523	
				40,397	$5 \cdot 10^{-6}$	4.6328	1.9572	
				160,797	10^{-6}	4.6444	1.9584	
Case 2	$5 \cdot 10^4$	0.01	1	437	$5 \cdot 10^{-5}$	6.7741	3.3319	Mean values
				2,597	$5 \cdot 10^{-5}$	7.0020	2.8477	
				10,197	10^{-5}	7.1591	2.7831	
				40,397	$5 \cdot 10^{-6}$	7.2786	2.7946	
				160,797	10^{-6}	7.3123	2.7991	

Note: Since Case 2 does not exhibit steady state, a mean value over one oscillation period is given

Table I.
Discretization parameters and principal results

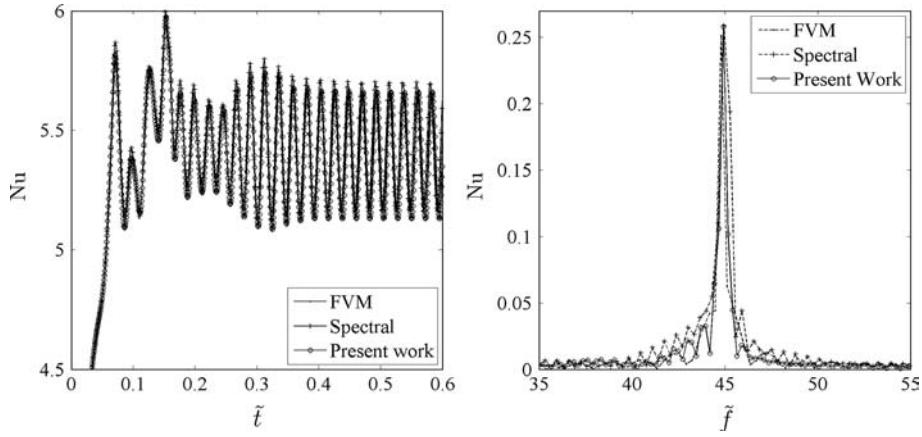

Figure 4.
Comparison case: left: hot side mean Nusselt number as a function of dimensionless time; right: hot side mean Nusselt number as a function of dimensionless frequency

plots are plotted on the left figure. The temporal development of the hot side mean Nusselt number is presented on the right figure. In Figure 6 the streamlines and the temperature contour plots for case 2 at different times during one oscillation are presented. In Figure 7 the hot side mean Nusselt number temporal development and in Figure 8 its representation in the frequency domain are presented, where $\tilde{f}$ stands for dimensionless frequency. One can observe from Figure 6 an almost same maximum flow intensity during oscillations. One can see from Figure 7 that increase of the number of the computational nodes also increases the amplitude of the oscillations. Both cases show good convergent behaviour with respect to the number of the discretization nodes (Figure 9). In case 2 it is

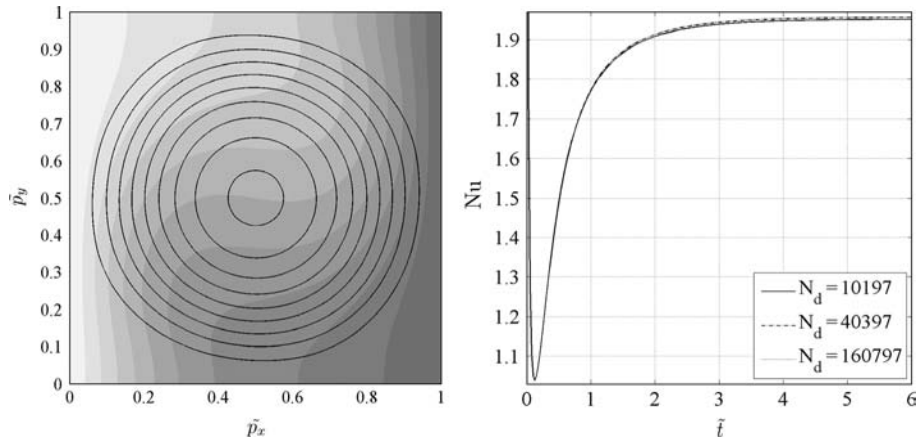

Figure 5.
Case 1: left: steady state streamlines (stream step 0.5) and temperature contours (contour step 0.1); right: hot side mean Nusselt number as a function of dimensionless time

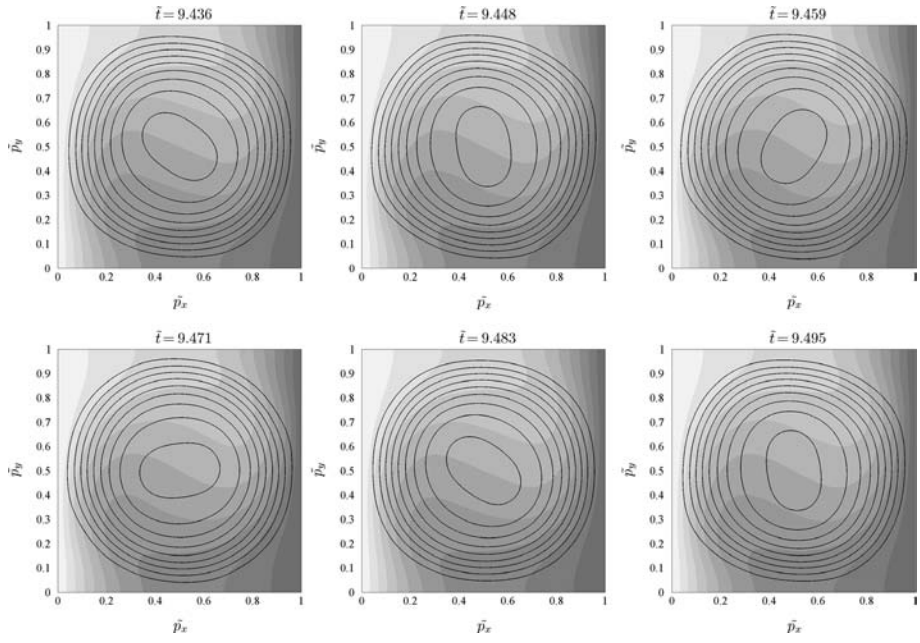

Figure 6.
Case 2: streamlines (stream step 0.8) and temperature contours (contour step 0.1) as a function of dimensionless time during one oscillation period

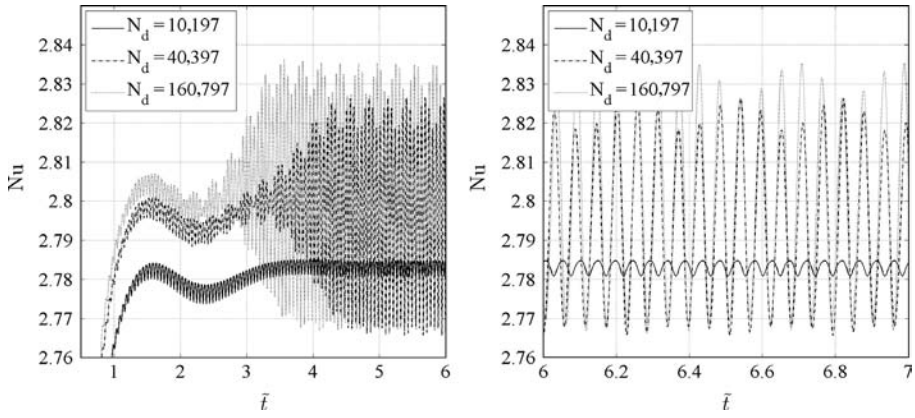

Figure 7.
Case 2: hot side mean Nusselt number as a function of dimensionless time

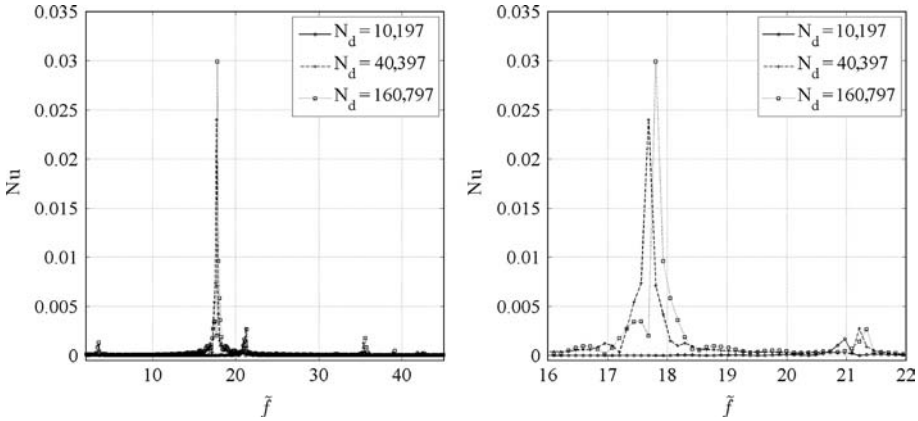

Figure 8.
Case 2: hot side mean Nusselt number as a function of the number of the domain nodes in frequency domain

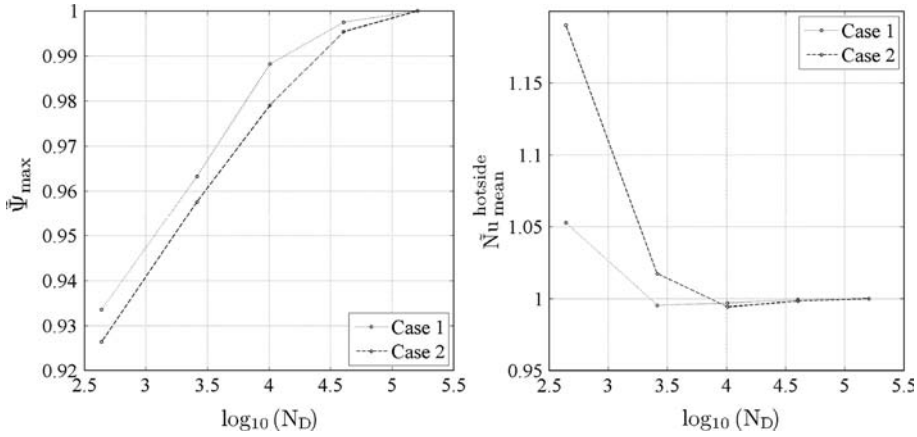

Figure 9.
Maximal streamfunction (left) and hot side mean Nusselt number (right) as a function of the number of domain nodes, where all quantities are normalized to one at the finest calculation

evident that using too coarse nodal distribution the important part of the solution can be missed as with the coarsest computation the strongest oscillation is not captured. The oscillation is more pronounced with the increasing number of the nodes. The oscillations are fully developed after initial transient which ends roughly at $\tilde{t} \sim 4.5$.

The oscillations in case 2 are result of a balance between the buoyancy and shear stress forces.

5. Conclusions

In the present paper we demonstrate the application of extremely simple and intuitive meshless numerical approach towards solution of transient thermo-fluid problems. The first two numerical problems from the spectra of recent solidification oriented benchmark call are treated. The low Prandtl number natural convection in a closed domain is solved with the proposed numerical solution procedure. Two cases are considered; one with steady state and another with oscillatory solution. In both situations we show good convergence behaviour. Until now, no other reference solution exists of the treated cases. In addition, we compare the present numerical approach on the treated oscillatory case and show excellent agreement with more common global numerical approaches. We show that in oscillatory case the coarse nodal distributions miss relevant physical behaviour. In our recent related work we research application of adaptive nodal distribution in connection with the method used in this paper (Kosec *et al.*, 2011). More involved solidification benchmark call tests will be attempted by this adaptive numerical approach. The future work will also be focused on a parallel implementation of current solver as we already achieve good speedups with straightforward OpenMP based parallelization. Further steps will be taken in a GPU and MPI based parallelization schemes.

References

Ahmad, N., Combeau, H., Desbiolles, J.L., Jalanti, T., Lesoult, G., Rappaz, J., Rappaz, M. and Stomp, C. (1998), "Numerical simulation of macrosegreation: a comparison between finite volume method and finite element method predictions and a confrontation with experiments", *Metallurgical and Materials Transactions*, Vol. A29, p. 617.

Amimul, A. (2011), *Convection and Conduction Heat Transfer*, Intech, Rijeka.

Arcidiacono, S. and Ciofalo, M. (2001), "Low-Prandtl number natural convection in volumetrically heated rectangular enclosures III. Shallow cavity, AR=0.25", *International Journal of Heat and Mass Transfer*, Vol. 44, pp. 3035-65.

Arcidiacono, S., Di Piazza, I. and Ciofalo, M. (2001), "Low-Prandtl number natural convection in volumetrically heated rectangular enclosures II. Square cavity, AR=1", *International Journal of Heat and Mass Transfer*, Vol. 44, pp. 537-50.

Atluri, S.N. and Shen, S. (2002a), "The meshless local Petrov-Galerkin (MLPG) method: a simple & less-costly alternative to the finite element and boundary element methods", *CMES: Computer Modeling in Engineering & Sciences*, Vol. 3, pp. 11-52.

Atluri, S.N. and Shen, S. (2002b), *The Meshless Method*, Tech Science Press, Encino.

Bellet, M., Combeau, H., Fautrelle, Y., Gobin, D., Rady, M., Arquis, E., Budenkova, O., Dussoubs, B., Duterrail, Y., Kumar, A., Gandin, C.A., Goyeau, B., Mosbah, S. and Zaloznik, M. (2009), "Call for contributions to a numerical benchmark problem for 2D columnar solidification of binary alloys", *International Journal of Thermal Sciences*, Vol. 48, pp. 2013-16.

Buhmann, M.D. (2000), *Radial Basis Functions*, Cambridge University Press, Cambridge.

Chen, W. (2002), "New RBF collocation schemes and kernel RBFs with applications", *Lecture Notes in Computational Science and Engineering*, Vol. 26, pp. 75-86.

Cless, C.M. and Prescott, P.J. (1996a), "Effect of time marching schemes on predictions of oscillatory natural convection", *Numerical Heat Transfer*, Vol. A29, pp. 575-97.

Cless, C.M. and Prescott, P.J. (1996b), "Effect of time varying thermal boundary conditions on oscillatory natural convection of a low-Prandtl-number fluid", *Numerical Heat Transfer*, Vol. A29, pp. 645-69.

Crunkleton, D.W., Narayanan, R. and Anderson, T.J. (2006), "Numerical simulations of periodic flow oscillations in low Prandtl number fluids", *International Journal of Heat and Mass Transfer*, Vol. 49, pp. 427-38.

de Vahl Davis, G. (1983), "Natural convection of air in a square cavity: a bench mark numerical solution", *International Journal for Numerical Methods in Fluids*, Vol. 3, pp. 249-64.

Di Piazza, I. and Ciofalo, M. (2001), "Low-Prandtl number natural convection in volumetrically heated rectangular enclosures II. Slender cavity, AR=4", *International Journal of Heat and Mass Transfer*, Vol. 43, pp. 3027-51.

Divo, E. and Kassab, A.J. (2007), "Localized meshless modeling of natural-convective viscous flows", *Numerical Heat Transfer*, Vol. B129, pp. 486-509.

Fasshauer, G. (2006), "Radial basis functions and related multivariate meshfree approximation methods: theory and applications – preface", *Computers & Mathematics with Applications*, Vol. 51, pp. 1223-366.

Franke, J. (1982), "Scattered data interpolation: tests of some methods", *Mathematics of Computation*, Vol. 48, pp. 181-200.

Gobin, D. and Le Quéré, P. (2000), "Melting from an isothermal vertical wall, synthesis of a numerical comparison excercise", *Computer Assisted Mechanics and Engineering Sciences*, Vol. 7, pp. 289-306.

Gu, G.R. and Liu, Y.T. (2005), *An Introduction to Meshfree Methods and Their Programming*, Springer, Dordrecht.

Hong, C.P. (2004), *Computer Modelling of Heat and Fluid Flow Materials Processing*, Institute of Physics Publishing, Bristol.

Kansa, E.J. (1990a), "Multiquadrics – a scattered data approximation scheme with application to computational fluid dynamics, part I", *Computers and Mathematics with Applications*, Vol. 19, pp. 127-45.

Kansa, E.J. (1990b), "Multiquadrics – a scattered data approximation scheme with application to computational fluid dynamics, part II", *Computers and Mathematics with Applications*, Vol. 19, pp. 147-61.

Kosec, G. and Šarler, B. (2008), "Solution of thermo-fluid problems by collocation with local pressure correction", *International Journal of Numerical Methods for Heat & Fluid Flow*, Vol. 18, pp. 868-82.

Kosec, G. and Šarler, B. (2009), "Solution of phase change problems by collocation with local pressure correction", *CMES: Computer Modeling in Engineering & Sciences*, Vol. 47, pp. 191-216.

Kosec, G., Založnik, M., Šarler, B. and Combeau, H. (2011), "A meshless approach towards solution of macrosegregation phenomena", *CMC: Computers, Materials, & Continua*, Vol. 580, pp. 1-27.

Liu, G.R. (2003), *Mesh Free Methods*, CRC Press, Boca Raton, FL.

Lorbiecka, A.Z. and Šarler, B. (2010), "Simulation of dendritic growth with different orientation by using the point automata method", *CMC: Computers, Materials, & Continua*, Vol. 18, pp. 69-103.

Malan, A.G. and Lewis, R.W. (2011), "An articial compressibility CBS method for modelling heat transfer and fluid flow in heterogeneous porous materials", *International Journal for Numerical Methods in Engineering*, Vol. 87, pp. 412-23.

Massarotti, N., Nithiarasu, P. and Zienkiewicz, O.C. (1998), "Characteristic-based-split (CBS) algorithm for incompressible flow problems with heat transfer", *International Journal of Numerical Methods for Heat and Fluid Flow*, Vol. 8, p. 969.

Mohamad, A.A. and Viskanta, R. (1991), "Transient natural convection of low-Prandtl-number fluids in a differentially heated cavity", *International Journal of Numerical Methods in Fluids*, Vol. 13, pp. 61-81.

Monaghan, J.J. (1988), "An introduction to SPH", *Computer Physics Communications*, Vol. 48, pp. 89-96.

Nakano, A., Ozoe, H. and Churchill, S.W. (1998), "Numerical computation of natural convection for a low-Prandtl-number fluid in a shallow rectangular region heated from below", *Chemical Engineering Journal*, Vol. 71, pp. 175-82.

Pesso, T. and Piva, S. (2009), "Laminar natural convection in a square cavity: low Prandtl numbers and large density differences", *International Journal of Heat and Mass Transfer*, Vol. 52, pp. 1036-43, available at: www.sciencedirect.com/science/article/pii/S0017931008004067

Rahman, M.M. and Siikonen, T. (2008), "An articial compressibility method for viscous incompressible and low Mach number flows", *International Journal for Numerical Methods in Engineering*, Vol. 75, pp. 1320-40.

Sammouda, H., Belghith, A. and Surry, C. (1999), "Finite element simulation of transient natural convection of low-Prandtl-number fluids in heated cavity", *International Journal of Numerical Methods for Heat and Fluid Flow*, Vol. 9 No. 5, pp. 612-24.

Šarler, B. (2007), *From Global to Local Radial Basis Function Collocation Method for Transport Phenomena*, Springer, Berlin, pp. 257-82.

Šarler, B. and Vertnik, R. (2006), "Meshfree explicit local radial basis function collocation method for diffusion problems", *Computers and Mathematics with Applications*, Vol. 51, pp. 1269-82.

Šterk, M. and Trobec, R. (2008), "Meshless solution of a diffusion equation with parameter optimization and error analysis", *Engineering Analysis with Boundary Elements*, Vol. 32, pp. 567-77.

Traivivatana, S., Boonmarlert, P., Thee, P., Phongthanapanich, S. and Dechaumphai, P. (2007), "Combined adaptive meshing technique and characteristic-based split algorithm for viscous incompressible flow analysis", *Applied Mathematics and Mechanics*, Vol. 28, pp. 1163-72.

Trobec, R., Šterk, M. and Robič, B. (2009), "Computational complexity and parallelization of the meshless local Petrov-Galerkin method", *Computers & Structures*, Vol. 87, pp. 81-90.

Vertnik, R. and Šarler, B. (2006), "Meshless local radial basis function collocation method for convective-diffusive solid-liquid phase change problems", *International Journal of Numerical Methods for Heat & Fluid Flow*, Vol. 16, pp. 617-40.

Vertnik, R., Šarler, B. and Senčič, B. (2011), "Solution of macrosegregation in continuously cast billets by a meshless method", paper presented at The 3rd International Conference on Advances in Solidification Processes.

Wang, J.G. and Liu, G.R. (2002), "A point interpolation meshless method based on radial basis functions", *International Journal for Numerical Methods in Engineering*, Vol. 54, pp. 1623-48.

Xiaohua, W., Yingjie, W. and Xinrong, S. (2009), "Numerical investigation of the first bifurcation for natural convection of fluids enclosed in a 2D square cavity with Pr lower than 1.0", *Energy Conversion and Management*, Vol. 50, pp. 2504-12.

Xin, S. and Le Quere, P. (2002), "An extended chebyshev pseudo – spectral benchmark for the 8:1 differentially – heated cavity", *International Journal of Numerical Methods in Fluids*, Vol. 40, pp. 981-98.

Založnik, M., Xin, S. and Šarler, B. (2005), "Verification of a numerical model of macrosegregation in direct chill casting", *International Journal of Numerical Methods for Heat & Fluid Flow*, Vol. 18, pp. 308-24.

Further reading

Kosec, G. and Šarler, B. (2011), "H-adaptive local radial basis function collocation meshless method", *Computers, Materials & Continua*, Vol. 26, pp. 227-54.

Corresponding author

Božidar Šarler can be contacted at: bozidar.sarler@ung.si